

Single-pulse characteristics of the Xe(L) amplifier on the Xe³⁵⁺ (3d→2p) transition array at $\lambda \cong 2.86 \text{ \AA}$

This article has been downloaded from IOPscience. Please scroll down to see the full text article.

2006 J. Phys. B: At. Mol. Opt. Phys. 39 L313

(<http://iopscience.iop.org/0953-4075/39/17/L01>)

View [the table of contents for this issue](#), or go to the [journal homepage](#) for more

Download details:

IP Address: 38.107.179.239

The article was downloaded on 26/05/2012 at 11:44

Please note that [terms and conditions apply](#).

LETTER TO THE EDITOR

Single-pulse characteristics of the Xe(L) amplifier on the Xe³⁵⁺ (3d→2p) transition array at $\lambda \cong 2.86 \text{ \AA}$

Alex B Borisov¹, Xiangyang Song¹, Ping Zhang¹, John C McCorkindale¹, Shahab F Khan¹, Richard DeJonghe¹, Sankar Poopalasingam¹, Ji Zhao¹, Keith Boyer¹ and Charles K Rhodes^{1,2,3,4}

¹ Laboratory for X-Ray Microimaging and Bioinformatics, Department of Physics, University of Illinois at Chicago, Chicago, IL 60607-7059, USA

² Department of Bioengineering, University of Illinois at Chicago, Chicago, IL 60607-7052, USA

³ Department of Computer Science, University of Illinois at Chicago, Chicago, IL 60607-7042, USA

⁴ Department of Electrical and Computer Engineering, University of Illinois at Chicago, Chicago, IL 60607-7053, USA

Received 15 May 2006, in final form 7 July 2006

Published 14 August 2006

Online at stacks.iop.org/JPhysB/39/L313

Abstract

The triple comparison of (1) single-pulse spectral data, recorded with a CCD-equipped von Hámos spectrometer both axially and transversely; (2) axially measured time-integrated spectra registered on a film and (3) single-pulse x-ray images of the morphology of the self-trapped plasma channel, recorded simultaneously with the single-pulse spectra, establishes several leading characteristics of the saturated amplification observed on the Xe³⁵⁺ transition array at $\lambda \cong 2.86 \text{ \AA}$. The chief findings are (α) absolute positive correlation of amplification with the formation of a plasma channel, (β) a perfect spectral match of the amplified transitions in the comparison of axially recorded single-pulse and time-integrated film data and (γ) exact spectral correspondence of both the axially registered single-pulse and time-integrated film data with single-pulse transversely measured spectra exhibiting deep spectral hole burning at the position of the Xe³⁵⁺ array.

1. Introduction

The recent observation [1–4] of strong amplification on multikilovolt ($\sim 4400 \text{ eV}$) Xe(L) hollow atom transitions [5, 6] in the $\sim 2.9 \text{ \AA}$ spectral region in stable ultra-intense relativistic plasma channels [7–13] is a direct consequence of the ability to produce a dense ensemble of highly excited states in an ordered way. The full complement of attributes canonically characteristic of a saturated amplifier was experimentally observed [1–3]. Specifically, they are (1) sharp spectral narrowing, (2) detection of a spatially narrow directed beam ($\delta\theta_x \cong 100\text{--}200 \text{ \mu rad}$), (3) dramatic increase in the amplitude of the emission and the development of

an intense output ($\geq 10^6$ enhancement) and (4) observation of deep spectral hole burning [2, 4] on the inhomogeneously broadened spontaneous emission profile at wavelengths correlating exactly with the amplified transitions. This work presents the results of single-pulse measurements [2, 14] illustrating the characteristics of the amplification occurring specifically on the Xe^{35+} (3d \rightarrow 2p) transition array at $\lambda \cong 2.86 \text{ \AA}$. The exceptionally favourable efficiency exhibited by amplification on this line is highly evident from previous measurements that showed spectral hole burning descending to the instrumental noise level, an outcome demonstrating the achievement of full energy extraction from the amplifying channel.

2. Characteristic Xe(L) single-pulse spectra

Previous work [1] has demonstrated that single-pulse images of the self-trapped plasma channel, along which the Xe(L) amplification occurs, can be registered by observation with an x-ray pinhole camera of the Xe(M) radiation collaterally produced in the $\sim 1 \text{ keV}$ spectral region. This information on the channel morphology can be combined with the corresponding single-pulse axially recorded amplified Xe(L) spectra obtained simultaneously with a CCD-equipped von Hámós instrument [2]. These spectral data can be further compared with the axially directed time-integrated spectra recorded in prior experiments on a film. As demonstrated affirmatively below for the Xe(L) Xe^{35+} (3d \rightarrow 2p) transition array, the principal experimental findings are as follows: (1) the observation of amplification and channel formation are fully correlated positively; no channel legislates no amplification, (2) a precise match is found for the wavelength corresponding to the amplified lines in a comparison of both the axially recorded single-pulse and time-integrated film spectra, and (3) an exact spectral agreement is manifest in the correspondence of single-pulse axially recorded amplification of the Xe^{35+} transitions and the strong spectral hole burning observed [2] in single-pulse transversely recorded spectra.

2.1. Xe(L) characteristic spontaneous emission spectral profile

The Xe(L) hollow atom spontaneous emission [5, 6], produced principally by (3d \rightarrow 2p) transitions of the form



that arise from the irradiation of Xe clusters with intense 248 nm radiation, exhibits the characteristic spectrum shown in figure 1(a) for both single-pulse (CCD) [2] and time-integrated film [1, 3, 4] recordings. Both spectra illustrated in figure 1 correspond to experimental conditions for which no amplification occurs. Since amplification is barred without the formation of a self-trapped channel [1, 3], the spectral agreement shown by the comparison [14] of the single-pulse (CCD) and film observations, in alliance with the confirmation provided by figure 1(b) of the simultaneous absence of a channel corresponding to the single-pulse data, validates both the reproducibility of the emission spectrum and the operational response of the CCD-equipped von Hámós spectrograph. The hollow atom emission spans the $\lambda \sim 2.55\text{--}2.95 \text{ \AA}$ spectral region and consists of two spin-orbit components upon which several Xe^{q+} transition arrays [5, 6] are superimposed. Although the full band of the observed spectrum is composed of thousands of individual transitions, a local structure that can be identified with specific Xe^{q+} arrays remains evident.

The experimental configuration under which these studies have been conducted has been fully described in prior publications [1, 2]. The key parameters governing the production of the

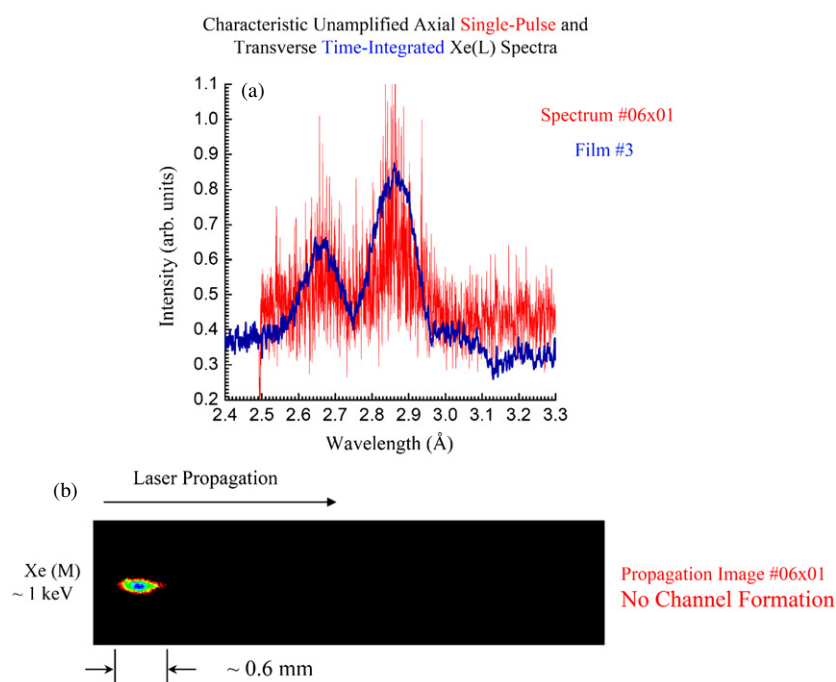


Figure 1. (a) Comparative film and single-pulse (CCD) recorded Xe(L) unamplified spontaneous emission spectral profiles produced by the irradiation of Xe clusters with femtosecond 248 nm excitation without plasma channel formation. Overlay of Xe(L) spectra recorded transversely (i) with a von Hámos spectrograph equipped with a film (blue contour, film #3) and (ii) on a single-pulse basis (red contour, spectrum #06×01) with the same instrument equipped with a CCD array in the film plane. A good agreement between the two recorded spectra is evident, an outcome validating both the reproducibility of the Xe(L) 3d→2p spectrum and the operational response of the CCD-equipped instrument. The noise level seen for the CCD recording is a characteristic of the instrumental response. The main transitions constituting the Xe(L) emission in the $\lambda \sim 2.5\text{--}3.0$ Å region are 3d→2p of the general form $2p^53d^n \rightarrow 2p^63d^{n-1}$ with $1 \leq n \leq 10$. For wavelengths $\lambda > 3.0$ Å, there exist 3s→2p transition arrays that can account for the relatively small difference between the film and CCD recordings. The splitting between the major and minor lobes arises principally from the spin–orbit interaction of the 2p vacancy; a small additional spin–orbit contribution arises from the 3d shell. The resolution of these films and CCD data is estimated to be ~ 4 eV. Both spectra correspond to conditions under which no amplifying channels are produced. (b) Single-exposure Xe(M) x-ray image of channel morphology taken with the same 248 nm pulse that produced spectrum #06×01 shown in panel (a). The image explicitly demonstrates that no confined propagating channel was formed and, consequently, no amplification was developed. This image of the Xe(M) radiation generated by the interaction was recorded with an x-ray pinhole camera having an aperture with a diameter of $25 \mu\text{m}$, a corresponding spatial resolution of $\sim 30 \mu\text{m}$ and a magnification of 1.1:1. The colour scale is defined by black (zero), red through violet ascending intensity and white (maximum).

data presented herein are summarized directly below. The femtosecond ultraviolet (248 nm) source used could deliver at a rate of 0.4 Hz a pulse with a maximal energy of ~ 400 mJ, a temporal duration of ~ 230 fs and a peak brightness of $\sim 8.5 \times 10^{21} \text{ W cm}^{-2} \text{ srad}^{-1}$. The gaseous xenon cluster (Xe_n) target was provided by a pulsed valve having an aperture of 1.5 mm that was operated at a maximum backing pressure of ~ 125 psia, a method that produced an average Xe density $\rho_{\text{Xe}} \sim 3\text{--}6 \times 10^{19} \text{ cm}^{-3}$ composed mainly of clusters in the vicinity of the nozzle in the evacuated chamber. The incident ultraviolet radiation was

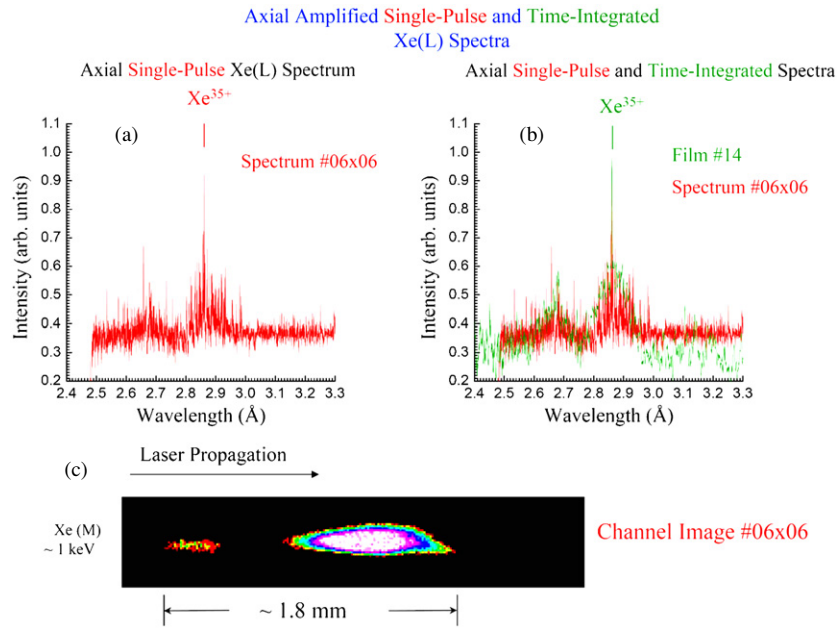


Figure 2. A comparison of axially measured Xe(L) spectra by both single-pulse (CCD) and film recordings with the simultaneous registration by x-ray imaging of the morphology of the plasma channel for the single-pulse data. (a) Single-pulse Xe(L) spectrum #06×06 showing a sharp peak at the position of the Xe³⁵⁺ array. On the basis of geometric considerations, the recorded enhancement of the Xe³⁵⁺ feature is estimated to be $\sim 1.5\text{--}3.0 \times 10^3$ over the strength of the spontaneous emission. (b) A comparison of spectrum #06×06, shown in panel (a), with film spectrum #14 that demonstrates the close overlap of the two corresponding enhanced features. (c) The plasma channel Xe(M) x-ray image corresponding to the single-pulse spectrum #06×06. The central gap in the image arises from the spatial resolution limit of the x-ray camera. As the channel becomes sufficiently narrow, the integrated exposure incident on the detector can fall below the dynamic range of the system. A channel length of ~ 1.8 mm is visible.

coupled to the cluster medium with an $f/3$ off-axis parabolic mirror, and the x-ray spectra were recorded in third-order diffraction with a von Hámós spectrograph equipped with a mica crystal and either a Kodak RAR 2492 film or a CCD located in the film plane.

2.2. Xe(L) single-pulse axially recorded spectra

The data illustrated in figures 2 and 3 present, in a triptych form, a brace of triple comparisons that show (a) the single-pulse axially measured Xe(L) spectrum, (b) a corresponding comparison of an axially recorded film spectrum with the single-pulse data appearing in panel (a) and (c) the channel Xe(M) x-ray image simultaneously registered with the single-pulse spectral data appearing in panel (a). For the spectra shown in panels (a) and (b), the axial alignment of the von Hámós spectrometer was set for satisfaction of the Bragg condition for the Xe³⁵⁺ transition at $\lambda \sim 2.86$ Å. The spectral comparison of the enhanced features shown in panel (b) demonstrates exact correspondence of the amplified wavelengths. It is particularly important to note that the spontaneous emission radiates into a solid angle

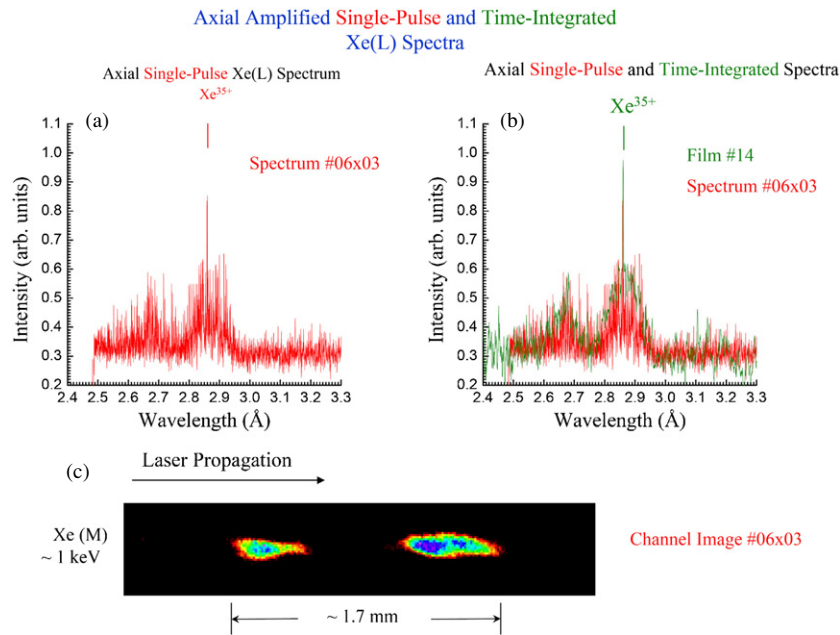


Figure 3. A comparison of axially measured Xe(L) spectra by both single-pulse (CCD) and film recordings with the simultaneous registration by x-ray imaging of the morphology of the plasma channel for the single-pulse data. (a) Single-pulse Xe(L) spectrum #06×03 showing a sharp peak at the position of the Xe³⁵⁺ array. The recorded enhancement of the Xe³⁵⁺ feature is estimated to be $\sim 1.5\text{--}3.0 \times 10^3$ over the strength of the spontaneous emission. (b) A comparison of spectrum #06×03, shown in panel (a), with film spectrum #14 that demonstrates the close overlap of the two corresponding enhanced features. (c) The plasma channel Xe(M) x-ray image corresponding to the single-pulse spectrum #06×03. The central gap in the image arises from the spatial resolution limit of the x-ray camera. As the channel becomes sufficiently narrow, the integrated exposure incident on the detector can fall below the dynamic range of the system. A channel length of ~ 1.7 mm is visible.

of 4π and is collected by the von Hámos spectrograph over a large angular region of ~ 300 mrad, while, in sharp contrast, the directed Xe³⁵⁺ signal represents a far smaller divergence of $\sim 100\text{--}200$ μ rad. As an immediate consequence of this geometric condition, it follows that the enhancements in signal strengths represented [1] for the Xe³⁵⁺ lines shown by the single-pulse data in figures 2 and 3 correspond to a factor of $\sim 1.5\text{--}3.0 \times 10^3$. Furthermore, since this estimate does not include the influence of imperfect alignment for the Bragg condition, these measurements perforce constitute lower bounds on the true magnitude of the amplification.

Additional single-pulse (CCD) data showing the character of the axially recorded amplification on the Xe³⁵⁺ transition array, together with the correspondences of these measurements with axial spectra taken with the film, are presented in an alternate triptych format in figures 4 and 5. Both single-pulse spectra (#10×01) and (#10×03) exhibit (i) strong amplification, (ii) perfect spectral correlation with the corresponding feature recorded axially with the film and (iii) excellent agreement with spectra (#06×06) and (#06×03), respectively illustrated in panel (a) of figures 2 and 3. Vice versa, all four of these single-pulse spectra display a clear contrast to the spectrum (#06×01) shown in figure 1(a), the result obtained without the formation of a plasma channel. Accordingly, these data firmly demonstrate full

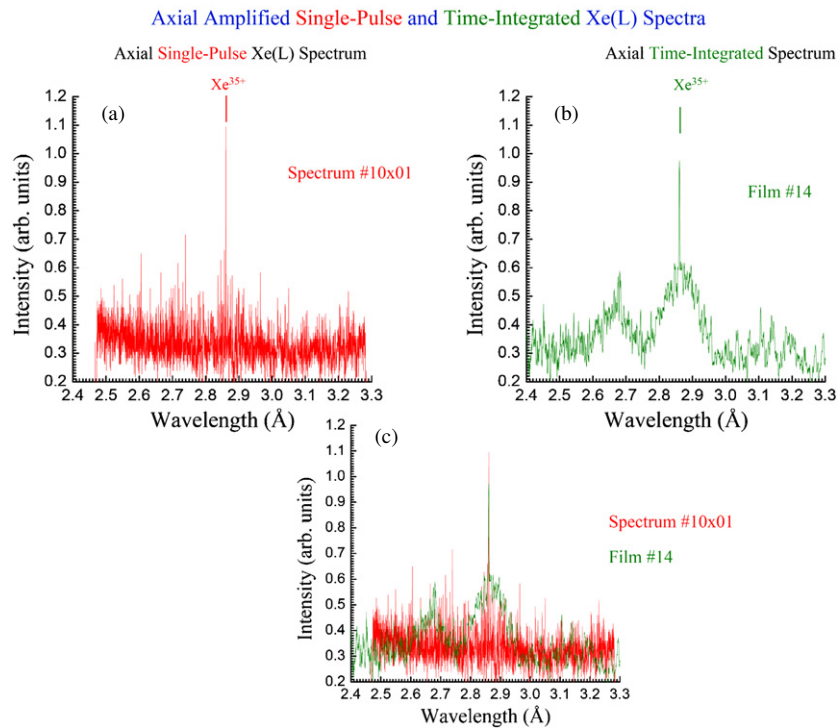


Figure 4. A comparison of axially measured Xe(L) spectra by both single-pulse (CCD) and film recordings. (a) Single-pulse Xe(L) spectrum #10×01 showing a sharp peak at the position of the Xe³⁵⁺ array. The recorded enhancement of the Xe³⁵⁺ feature is estimated to be minimally on the order of $\sim 1.5\text{--}3.0 \times 10^3$ over the strength of the spontaneous emission. The near absence of the characteristic double-lobed Xe(L) emission profile indicates that a very strong relative enhancement of the directed Xe³⁵⁺ signal is present. (b) Axially observed Xe(L) spectrum recorded on film (#14) showing a sharp enhancement of the transitions associated with the Xe³⁵⁺ array. In comparison to the Xe(L) spectrum transversely recorded on film #3, that is illustrated in figure 1(a), we note that the Xe(L) spectrum axially recorded on film #14 reveals slight differences in the detailed structure of the spectrum. An example is given by the small feature indicating enhancement at $\lambda \sim 2.68 \text{ \AA}$ in film #14. (c) A comparison of spectrum #10×01, shown in panel (a), with film spectrum #14 that demonstrates the precise overlap of the two corresponding enhanced features.

positive correlation of amplification in the presence of a self-trapped channel and perfect spectral correspondence of the amplified Xe³⁵⁺ transitions in the comparison of single-pulse (CCD) data and observations recorded on film.

2.3. Correlation of channel morphology with spectral hole burning on the Xe³⁵⁺ array

A chief signature of saturated amplification is the observation of spectral hole burning [1, 2]. As demonstrated above, the formation of a self-trapped plasma channel is a requisite for amplification [1]. Hence, channel formation and spectral hole burning on the Xe³⁵⁺ array should be positively and fully correlated in single-pulse measurements. The data presented in figure 6 demonstrate this expectation by showing (a) the deep spectral hole burning observed transversely to the axis of the channel in a single-pulse (CCD) spectrum that is centred on the

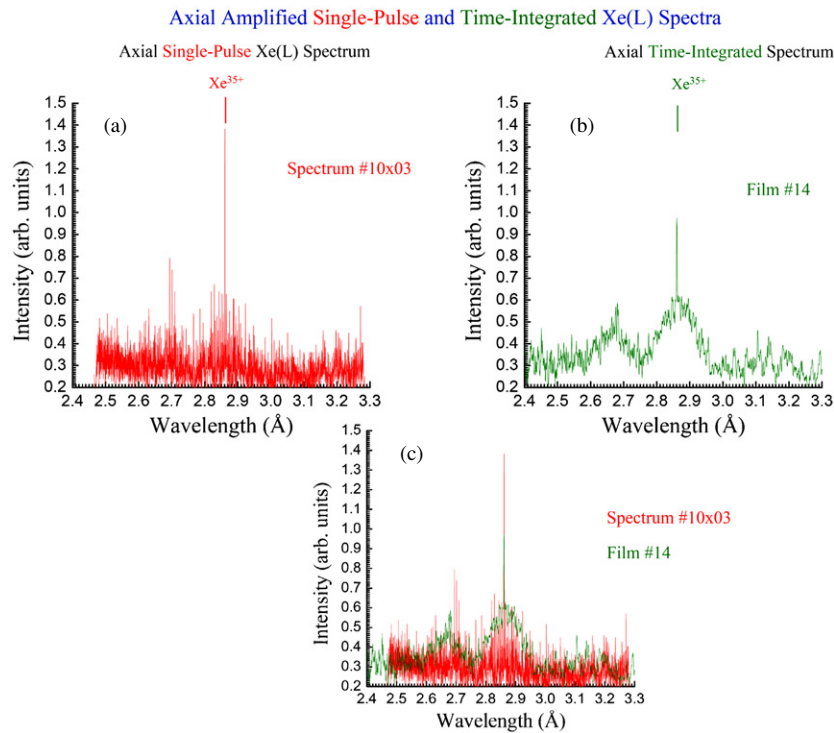


Figure 5. A comparison of axially measured Xe(L) spectra by both single-pulse (CCD) and film recordings. (a) Single-pulse Xe(L) spectrum #10×03 showing a sharp peak at the position of the Xe³⁵⁺ array. The recorded enhancement of the Xe³⁵⁺ feature is estimated to be $\sim 1.5\text{--}3.0 \times 10^3$ over the strength of the spontaneous emission. (b) Axially observed Xe(L) spectrum recorded on film (#14) showing a sharp enhancement of the transitions associated with the Xe³⁵⁺ array. (c) A comparison of spectrum #10×03, shown in panel (a), with film spectrum #14 that demonstrates the exact overlap of the two corresponding enhanced features.

wavelength of the Xe³⁵⁺ array recorded on the film and (b) the simultaneous formation of a self-trapped channel.

3. Conclusions

Single-pulse (CCD) measurements of axially and transversely recorded Xe(L) spectra, together with simultaneously registered single-pulse Xe(M) x-ray images of the morphology of the self-trapped plasma channel and time-integrated spectra observed axially with the film, have demonstrated several leading characteristics of the amplification occurring on the Xe³⁵⁺ transition array. The principal findings are (1) the full positive correlation of the observation of amplification with the formation of a plasma channel; no amplification develops without the simultaneous presence of a propagating channel, (2) a precise match for the wavelength of the amplified Xe³⁵⁺ array in the direct comparison of axially measured single-pulse and film spectra, and (3) exact spectral correspondence in the triple comparison of (i) the single-pulse axially recorded amplification, (ii) the single-pulse transversely observed occurrence of strong spectral hole burning, and (iii) axially registered time-integrated film data illustrating amplification.

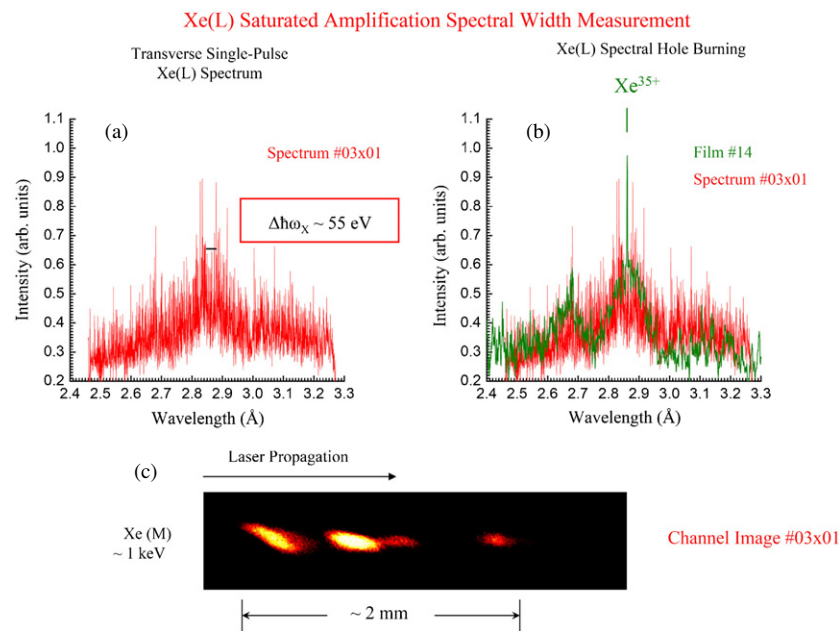


Figure 6. Single-pulse demonstration of the correlation of Xe(L) spectral hole burning on Xe³⁵⁺ array with the formation of an extended self-trapped plasma channel. (a) Single-pulse transversely observed Xe(L) spectrum #03x01 exhibiting strong spectral hole burning at the position of the Xe³⁵⁺ transition array. The width of the spectral gap is $\Delta\omega_x \cong 55 \text{ eV}$ and the signal descends to the noise level of the detector at $\lambda \cong 2.86 \text{ \AA}$. (b) A comparison of single-pulse data (#03x01) with an axially recorded film (#14) spectrum showing amplification on the Xe³⁵⁺ array that is centred on the hole-burned spectral gap at $\lambda \cong 2.86 \text{ \AA}$. (c) The plasma channel Xe(M) x-ray image corresponding to the single-pulse spectrum #03x01 shown in panel (a). A channel length of $\sim 2 \text{ mm}$ is visible. The unusual spatial configuration of the Xe(M) signal recorded arises from the dynamics of the propagating 248 nm pulse. This effect has been discussed in the previous work [10].

Acknowledgments

The authors would like to thank C Martin Stickley for his support and encouragement. CKR acknowledges fruitful discussions with Gerd Marowsky. The work was supported in part by a contract with the Naval Research Laboratory (N00173-03-1-6015) and the BAE Systems project.

References

- [1] Borisov A B, Song X, Frigeni F, Koshman Y, Dai Y, Boyer K and Rhodes C K 2003 Ultrabright multikilovolt coherent tunable x-ray source at $\lambda \sim 2.71\text{--}2.93 \text{ \AA}$ *J. Phys. B: At. Mol. Opt. Phys.* **36** 3433
- [2] Borisov A B, Davis J, Song X, Koshman Y, Dai Y, Boyer K and Rhodes C K 2003 Saturated multikilovolt x-ray amplification with Xe clusters: single-pulse observation of Xe(L) spectral hole burning *J. Phys. B: At. Mol. Opt. Phys.* **36** L285
- [3] Boyer K, Borisov A B, Song X, Zhang P, McCorkindale J C, Khan S, Dai Y, Kepple P C, Davis J and Rhodes C K 2005 Explosive supersaturated amplification on $3d \rightarrow 2p$ Xe(L) hollow atom transitions at $\lambda \sim 2.7\text{--}2.9 \text{ \AA}$ *J. Phys. B: At. Mol. Opt. Phys.* **38** 3055
- [4] Borisov A B, Song X, Zhang P, Dasgupta A, Davis J, Kepple P C, Dai Y, Boyer K and Rhodes C K 2005 Amplification at $\lambda \sim 2.8 \text{ \AA}$ on Xe(L) $2s2p$ double-vacancy states produced by 248 nm excitation of Xe clusters in plasma channels *J. Phys. B: At. Mol. Opt. Phys.* **38** 3935

- [5] Clark M W, Schneider D, DeWitt D, McDonald J W, Bruch R, Safronova U I, Tolstikhina I Yu and Schuch R 1993 Xe(L) and (M) x-ray emission following Xe^{44–48+} ion impact on Cu surfaces *Phys. Rev. A* **47** 3983
- [6] MacPherson A, Thompson B D, Borisov A B, Boyer K and Rhodes C K 1994 Multiphoton-induced x-ray emission at 4–5 keV from Xe atoms with multiple core vacancies *Nature* **370** 631
- [7] Borisov A B, Borovskiy A V, Korobkin V V, Prokhorov A M, Shiryayev O B, Shi X M, Luk T S, McPherson A, Solem J C, Boyer K and Rhodes C K 1992 Observation of relativistic and charge-displacement self-channeling of intense subpicosecond ultraviolet (248 nm) radiation in plasmas *Phys. Rev. Lett.* **68** 2309
- [8] Borisov A B, Borovskiy A V, Shiryayev O B, Korobkin V V, Prokhorov A M, Solem J C, Luk T S, Boyer K and Rhodes C K 1992 Relativistic and charge-displacement self-channeling of intense ultrashort laser pulses in plasmas *Phys. Rev. A* **45** 5830
- [9] Borisov A B, Shi X, Karpov V B, Korobkin V V, Solem J C, Shiryayev O B, McPherson A, Boyer K and Rhodes C K 1994 Stable self-channeling of intense ultraviolet pulses in underdense plasma, producing channels exceeding 100 Rayleigh lengths *J. Opt. Soc. Am. B* **11** 1941
- [10] Borisov A B, McPherson A, Thompson B D, Boyer K and Rhodes C K 1995 Ultrahigh power compression for x-ray amplification: multiphoton cluster excitation combined with nonlinear channeled propagation *J. Phys. B: At. Mol. Opt. Phys.* **28** 2143
- [11] Borisov A B, Longworth J W, Boyer K and Rhodes C K 1998 Stable relativistic/charge displacement channels in ultrahigh power density ($\sim 10^{21}$ W cm⁻³) plasmas *Proc. Natl Acad. Sci. USA* **95** 7854
- [12] Monot P, Auguste T, Gibbon P, Jakober F, Mainfray G, Dullieu A, Louis-Jacquet M, Malka G and Miquel J L 1995 Experimental demonstration of relativistic self-channeling of a multiterawatt laser pulse in an underdense plasma *Phys. Rev. Lett.* **74** 2953
- [13] Pukhov A 2003 Strong field interaction of laser radiation *Rep. Prog. Phys.* **66** 47
- [14] Boyer K, Borisov A B, Song X, Zhang P, McCorkindale J C, Khan S F, DeJonghe R and Rhodes C K 2006 Xe(L) coherent x-ray source at $\lambda \sim 2.9$ Å for biological nanoimaging *Superstrong Fields in Plasmas, AIP Conf. Proc.* vol 827 ed D Batani and M Lontano (Melville, NY: AIP) p 457